

High quality CVD diamond: a Raman scattering and photoluminescence study

M.G. Donato¹, G. Faggio¹, M. Marinelli², G. Messina^{1,a}, E. Milani², A. Paoletti², S. Santangelo¹, A. Tucciarone², and G. Verona Rinati²

¹ INFN, Dipartimento di Meccanica e Materiali, Facoltà di Ingegneria dell'Università, Località Feo di Vito, 89060 Reggio Calabria, Italy

² INFN, Dipartimento di Scienze e Tecnologie Fisiche ed Energetiche, Università di Roma Tor Vergata, via di Tor Vergata, 00133 Roma, Italy

Received 24 November 2000

Abstract. High quality synthetic diamonds were grown on single-crystal silicon by microwave plasma enhanced chemical vapour deposition (CVD). A careful optimisation of both the experimental setup and the growth parameters was necessary before that the achievement of the best results was made possible. The films were deposited using a CH₄-H₂ gas mixture at methane concentrations variable in the range 0.6–2.2%, while the substrate temperature was fixed at 750 °C. Raman spectroscopy and photoluminescence (PL) were utilised to monitor the quality of the deposited films and to study the spatial distribution of defects, respectively. Micro-Raman analysis shows that linewidths of the diamond peak lower than 2.4 cm⁻¹ can be easily measured at the growth surface, indicating that the crystalline quality of individual grains is comparable to that of the best natural diamonds. The excellent phase purity of the diamond microcrystals at the growth surface is witnessed by the complete absence of any non-diamond carbon feature and by a very weak luminescence background in the 1.6–2.4 eV spectral range. A worsening of the quality of the diamond particles is found moving from the growth surface towards the film-substrate interface. A photoluminescence feature at about 1.68 eV, commonly associated to Si impurities, is distinctly observed as the exciting laser beam is focused close to the interface. A progressive degradation of the global quality of the films is found with increasing methane concentration in the gas mixture, as witnessed by an increased PL background in the films grown at higher methane concentrations.

PACS. 81.05.Uw Carbon, diamond, graphite – 78.30.Am Elemental semiconductors and insulators – 78.55.Ap Elemental semiconductors

1 Introduction

Due to the unique combination of exceptional physical properties of natural diamond, in the last twenty years a considerable amount of work has been devoted all over the world to the growth of synthetic diamond by chemical vapour deposition (CVD) processes at low-pressures. The chief motivation of these research efforts has been the hope of producing, at low-cost, a high-quality material with a great variety of potential applications in microelectronics, optics, micromechanics and, more generally, in all those fields where advanced devices are required to operate in extreme environments. Nowadays, thanks to the maturation of the Microwave Plasma Enhanced Chemical Vapour Deposition (MWPECVD) technique, synthetic diamond films possessing all the outstanding physical properties of natural diamond can be

obtained in a controlled way. This opens the road to the realisation of devices fully exploiting the unique properties of diamond. However, compared to natural diamond or to single-crystal synthetic diamond obtained by high-pressure/high-temperature methods, CVD diamond films grown on non-diamond substrates are polycrystalline and generally contain a relatively high concentration of impurities and crystal defects. These undesired inclusions may significantly degrade their optical and electronic properties, actually limiting the development of new diamond devices. In this respect, the main technical challenge that the scientific community is called to face is to improve the intrinsic quality of individual diamond particles, reducing the density of crystal defects and impurities incorporated during the growth process. The possibility of producing high-quality films is thus strictly connected to a better understanding of the microscopic structure of the films. In this context, a key role is played by characterisation

^a e-mail: messina@unirc.it

studies which, clarifying the relationships among growth conditions and structural properties of the films, may promote the optimisation of the growth process.

Optical techniques as photoluminescence (PL) and Raman spectroscopy have proven to be powerful non-destructive tools for evaluating the quality of diamond samples. In particular, as impurities and defects generally possess electronic energy levels within the diamond band gap, PL spectroscopy is commonly used for studying the nature and the distribution of crystal defects and impurity-induced optical centres in diamond films. Raman spectroscopy represents one of the most useful diagnostic techniques used for characterising diamond films, since it allows a ready identification of the different carbon allotropes present in the sample. Natural diamond exhibits a single sharp line at 1332 cm^{-1} , having a full width at half maximum (FWHM) of about 2 cm^{-1} . Natural single-crystal graphite shows a single Raman peak at 1580 cm^{-1} , while an additional band, activated by the disorder, appears at about 1350 cm^{-1} in polycrystalline graphite. Amorphous carbon exhibits a broad asymmetric band centred around 1500 cm^{-1} , containing two or more overlapping components located between the two graphite bands [1]. All these features, together with others not well identified and a strong luminescence background, are generally found in the Raman spectrum of CVD diamond films [1–3]. In particular, the sharp line characteristic of the diamond structure is generally shifted with respect to 1332 cm^{-1} due to internal stress, and it is much broader than in natural diamond due to crystal defects or an inhomogeneous distribution of stress [4,5].

In this work we report on high quality diamond films grown on single-crystal silicon by MWPECVD using a $\text{CH}_4\text{-H}_2$ gas mixture. On the basis of the results of a previous systematic study of CVD samples grown using a $\text{CH}_4\text{-CO}_2$ gas mixture [6], a careful optimisation of both the experimental set-up and the growth parameters was carried out.

Raman spectroscopy and PL have been utilised to assess the quality of the deposited films and to investigate the defect formation. In particular, a detailed micro-Raman study shows that the diamond crystals on the growth surface have intrinsic quality comparable to that of unselected natural diamonds, as evidenced by Raman peaks at 1332 cm^{-1} narrower than 2.4 cm^{-1} . Although comparable linewidths have been previously measured on isolated CVD diamond particles, to the best of our knowledge, our linewidths take their place among the narrowest ever reported in continuous diamond films deposited onto non-diamond substrates.

Due to the columnar nature of CVD diamond growth, a worsening of the crystalline quality is found moving towards the film-substrate interface. In particular, the diamond peak broadens and a large PL band centred at $\sim 2\text{ eV}$, almost completely absent at the growth surface, is detected moving towards the substrate. In addition, a PL signal at about 1.68 eV is distinctly observed close to the interface, whose intensity progressively decreases moving towards the growth surface. Its depth dependence provides

further support to the conclusion that the 1.68 eV centre is related to Si impurities released by the substrate etched by the plasma at the initial stages of growth [7,8]. Independently of the gas mixture, the diamond films deposited at higher methane concentration show a more defective crystalline structure, as witnessed by the progressively increasing broadband PL at $\sim 2\text{ eV}$.

The high crystalline quality of these films has been independently assessed through their highly sensitive performance in UV radiation and α -particle detection [9,10]. A degradation of the detection performance of the films grown at higher methane concentrations is found, clearly expected on the basis of the structural characterisation.

2 Experimental

The diamond films used in this study were deposited by MWPECVD in a microwave reactor realised by a quartz tube of 50 mm diameter. The growth plasma was produced in the reaction chamber by excitation with 2.45 GHz microwaves from a 2 kW commercial magnetron. In order to increase the nucleation density of diamond particles, the *p*-type (100) silicon substrates were pretreated by scratching with $20\text{ }\mu\text{m}$ diamond power. The substrate size was typically in the range $5 \times 5 - 10 \times 10\text{ mm}^2$. Both $\text{CH}_4\text{-CO}_2$ and $\text{CH}_4\text{-H}_2$ gas mixtures were used as gaseous precursors during the deposition process. In order to minimise the impurity content in the film, ultra pure gases were used and, before introducing the gas mixture, a base pressure of about 10^{-6} mbar was achieved in the deposition chamber. During a typical deposition process, the total gas pressure was about 120 mbar , the gas flow rate was about 100 sccm , the microwave power was in the range $400\text{--}700\text{ W}$.

A careful optimisation of both the reactor geometry and the plasma energy density was necessary before achieving the best results. An automatic system was realised for accurately controlling the growth temperature, measured by an infrared optical pyrometer. The signal from the pyrometer is sent to a computer that adjust the output power of the microwave generator in order to maintain the substrate temperature to the pre-fixed value. The geometry of the deposition reactor was modified in order to minimize the microwave-power losses. An appropriate water-cooling of the substrate holder was realised in order to ensure an accurate control of the substrate temperature. After the optimisation of the experimental setup, the $\text{CH}_4\text{-H}_2$ gas mixture was used, owing to the much lower deposition rates with respect to the $\text{CH}_4\text{-CO}_2$ mixture ($\sim 0.9\text{ }\mu\text{m/h}$ against $\sim 4\text{ }\mu\text{m/h}$).

The Raman scattering measurements were performed at room temperature on an Instrument S.A. Ramanor U1000 double monochromator, equipped with a microscope Olympus BX40 for micro-Raman sampling and with an electrically cooled Hamamatsu R943-02 photomultiplier for photon-counting detection. The 514.5 nm line of an Ar^+ ion laser (Coherent Innova 70) was used to excite Raman scattering; the laser power was about 10 mW at the sample surface. Using an X100 objective, the laser

Table 1. Growth conditions and Raman parameters for the four samples of Figure 1.

Sample	T_s ($^{\circ}\text{C}$)	CH_4 (%)	FWHM (cm^{-1})	$A_{\text{ND}}/A_{\text{D}}$	Slope ($\text{cps}/\text{cm}^{-1}$)
A	850	48.1	8.7	0.28	1.57
B	850	50.0	5.2	0.34	2.55
C	750	48.1	4.7	0.06	1.45
D	750	52.0	2.4	0.15	2.94

beam was focused to a diameter of about $1\ \mu\text{m}$. Its position on the sample surface was monitored by a video camera. A depth resolution of about $2\ \mu\text{m}$ was obtained with a confocal aperture of $100\ \mu\text{m}$. A spectral slit width of $\sim 0.9\ \text{cm}^{-1}$ (slit width = $100\ \mu\text{m}$) was used. All components of the micro-Raman spectrometer were fixed on a vibration damped optical table. Micro-photoluminescence ($\mu\text{-PL}$) measurements were carried out at room temperature by using the same experimental set-up used for micro-Raman spectroscopy. The $514.5\ \text{nm}$ green line ($2.41\ \text{eV}$) of the argon-ion laser was used to excite luminescence; the spectra were taken in the region $1.6\text{--}2.4\ \text{eV}$ ($100\text{--}6500\ \text{cm}^{-1}$ in a relative scale).

3 Results before optimisation

Raman and PL spectroscopy have been utilised to compare the quality of the CVD diamond films deposited before and after the optimisation of both the experimental set-up and the growth parameters. The effect of the deposition temperature and the methane concentration on the film structural properties was clearly established in a previous systematic study carried out on CVD diamond samples grown using a $\text{CH}_4\text{-CO}_2$ gas mixture [6].

Figure 1 shows the micro-Raman spectra taken at the growth surface of four samples grown at two different substrate temperatures ($T_s = 750\ ^{\circ}\text{C}$ and $T_s = 850\ ^{\circ}\text{C}$) and at different methane concentrations. Their crystalline quality and phase purity were assessed, respectively, by measuring FWHM of the diamond Raman line at $1332\ \text{cm}^{-1}$ and by calculating the ratio of the amplitude A_{ND} of the non-diamond carbon band at about $1500\ \text{cm}^{-1}$ to the amplitude A_{D} of the diamond peak. The growth parameters of the four samples of Figure 1 are summarised in Table 1, together with the quality factors FWHM and $A_{\text{ND}}/A_{\text{D}}$. The average slope of the spectrum, evaluated in the interval $800\text{--}2000\ \text{cm}^{-1}$ and reported in last column of the table, gives qualitative information about the sample photoluminescence.

Decreasing the deposition temperature from 850 to $750\ ^{\circ}\text{C}$ causes a narrowing of the diamond line and a lowering of the large non-diamond band around $1500\ \text{cm}^{-1}$. This indicates that better crystalline quality and higher phase purity are obtained at lower substrate temperature. At both substrate temperatures, the non-diamond to diamond ratio increases with increasing methane concentration, which indicates that the incorporation of graphitic and amorphous carbon within the individual grains is progressively greater at higher CH_4 con-

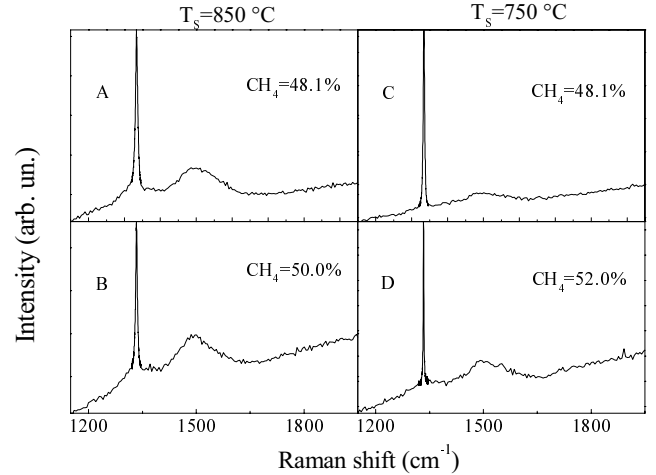


Fig. 1. Micro-Raman spectra at the growth surface of diamond samples grown with the $\text{CH}_4\text{-CO}_2$ gas mixture. The deposition conditions of the four samples (A, B, C, D) and the fitting parameters are reported in Table 1.

centration [11,12]. The lower phase purity of the films deposited at higher methane concentrations is related to the deposition rate, which increases monotonically with increasing methane concentration.

The $\mu\text{-PL}$ spectra of all the samples grown using the $\text{CH}_4\text{-CO}_2$ gas mixture exhibit a quite smooth broad band centred at about $2\ \text{eV}$ ($\sim 3000\ \text{cm}^{-1}$ in a relative scale), frequently observed in CVD diamond films under various excitation conditions [7,8,13–16]. Figure 2 compares the $\mu\text{-PL}$ spectra of two diamond samples grown at different methane concentrations ((a) 47.4% and (b) 50.0%) and having, consequently, different phase purity qualitatively measured by the $A_{\text{ND}}/A_{\text{D}}$ ratio. The intensity of the broadband PL increases going from the sample of higher purity to that of lower purity. In particular, the ratio $A_{\text{PL}}/A_{\text{D}}$ of the PL amplitude to the diamond line amplitude increases of almost a factor of three. Other authors have previously reported a correlation between broadband PL and phase purity [7,8]. It has been suggested that the sp^2 phase, present in disordered configuration in the diamond film, may introduce a continuous distribution of states within the optical band gap of diamond. The broad PL band at about $2\ \text{eV}$ has been attributed to the optical transitions in the in-gap state distribution. Although the spectra of Figures 1 and 2 evidence traces of non-diamond carbon even within diamond crystals at the growth surface, the qualitative figures of merit of Table 1

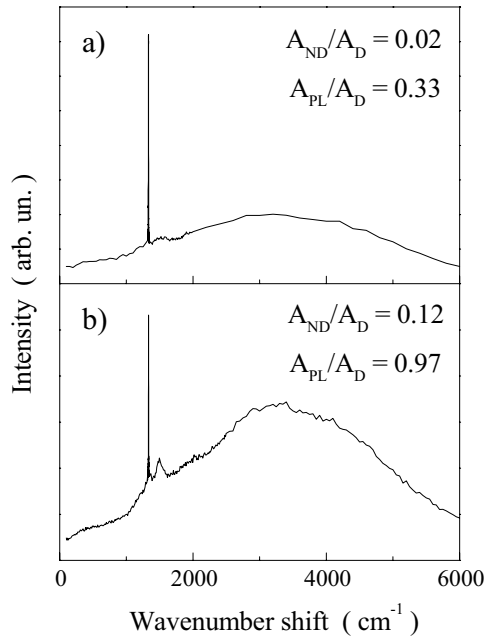


Fig. 2. Micro-PL spectra of two samples grown at different methane concentrations ($\text{CH}_4\text{-CO}_2$ gas mixture): (a) $\text{CH}_4 = 47.4\%$; (b) $\text{CH}_4 = 50\%$.

indicate that the samples grown using the $\text{CH}_4\text{-CO}_2$ gas mixture are of quite good quality.

4 Results after optimisation

New diamond samples were grown after modifying the deposition reactor in such a way as to avoid loss of microwave power in the vertical section of the NIRIM-type reactor, thus optimising the coupling of the microwaves to the plasma. The previously utilised $\text{CH}_4\text{-CO}_2$ gas mixture was replaced by the $\text{CH}_4\text{-H}_2$ one, which leads to much lower deposition rates, while the substrate temperature was fixed at 750°C . Thanks to the more efficient cooling of the substrate the microwave power could be increased from $\sim 400\text{ W}$ to $\sim 700\text{ W}$ without raising the substrate temperature. In this way, the energy density in the plasma correspondingly increased by approximately a factor of two. The optical microscope inspection showed that the obtained films consist of diamond crystallites having dimensions in the range $5\text{--}20\ \mu\text{m}$. The film preferential orientation changed from random to (110) with increasing the methane concentration from 0.6 to 2.2%. The film thickness, evaluated through a SEM image of the cross section, correspondingly varied from 30 to $50\ \mu\text{m}$, for a fixed deposition time of 45 hours. The corresponding growth rates changed from $0.7\ \mu\text{m/h}$ (for the 0.6% sample) to $1.1\ \mu\text{m/h}$ (for the 2.2% sample).

4.1 Growth surface

Figure 3 shows the $\mu\text{-PL}$ spectrum taken on the growth surface of a diamond sample grown at 0.6% CH_4 in H_2 .

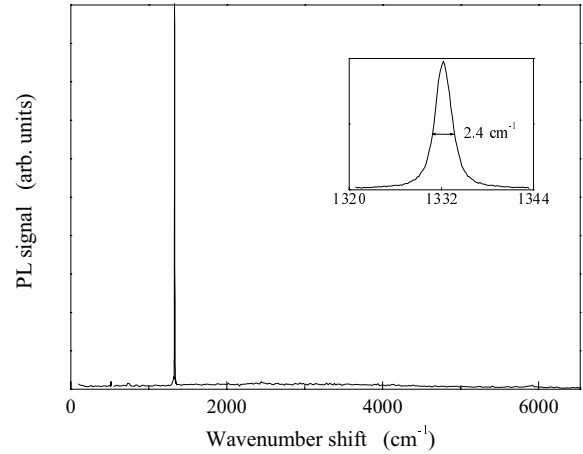


Fig. 3. Micro-PL spectrum at the growth surface of a sample deposited using the $\text{CH}_4\text{-H}_2$ gas mixture with 0.6% CH_4 . The diamond Raman line is shown in the inset and its FWHM is also indicated.

The spectrum is dominated by the sharp diamond Raman line at about $1332\ \text{cm}^{-1}$, whose intensity is comparable to that measured in a single-crystal diamond used as reference sample ($\text{FWHM} \cong 2\ \text{cm}^{-1}$, peak position $1332\ \text{cm}^{-1}$). Its Lorentzian FWHM of only $2.4\ \text{cm}^{-1}$ clearly indicates the very good crystalline quality of the sample. A so narrow linewidth is not exceptional at the growth surface of the samples grown under optimised conditions. Concerning this, it is worth noting that the FWHM values reported in this work have not been corrected for the slit-induced broadening. Actually micro-Raman measurements carried out on a great deal of grains with different morphology show linewidths ranging from 2.1 to about $3\ \text{cm}^{-1}$, while peak positions between 1332 and $1333\ \text{cm}^{-1}$ indicate a low amount of residual stress. Furthermore, at variance with the samples grown before optimisation [5], no splitting of the diamond line has been observed, usually attributed to the presence of large anisotropic stresses within the film [4,17–19].

Linewidths as narrow as $2.1\ \text{cm}^{-1}$ have been recently measured in single-crystal diamond grown by CVD on single-crystal diamond substrates [20]. Diamond peak widths comparable to ours have been previously measured both in large isolated CVD diamond particles ($\sim 100\ \mu\text{m}$, $\text{FWHM} = 2.3\ \text{cm}^{-1}$) [21] and in small isolated CVD diamond particles ($\sim 2\ \mu\text{m}$, $\text{FWHM} = 2.7\ \text{cm}^{-1}$) [22]. As for CVD diamond films, diamond-peak linewidths comparable to ours have been recently reported by some authors [23–26]. In particular, Coe *et al.* [24] report on De Beers CVD diamond films (thickness $\sim 1\ \text{mm}$) with FWHM of approximately $3\ \text{cm}^{-1}$; Jany *et al.* [25] show FWHM values as low as $2.6\ \text{cm}^{-1}$ both in $20\ \mu\text{m}$ thick films and in a $100\ \mu\text{m}$ thick film; Meier [26] measures linewidths ranging from 2.1 to $2.9\ \text{cm}^{-1}$ on $\sim 500\ \mu\text{m}$ thick films intended for the implementation of particle detectors. From these literature data, we can say that the FWHM values reported in the present work are quite

interesting, especially considering the relatively low thickness of our samples.

The very weak PL band centred at about 2900 cm^{-1} , the complete absence of any non-diamond carbon feature around 1500 cm^{-1} and of any other impurity feature demonstrate the very high phase purity achieved in the new samples. In particular, the amplitude of the diamond peak is more than sixty times greater than that of the broad PL band. The comparison with Figure 2a shows that the $A_{\text{PL}}/A_{\text{D}}$ ratio ($\cong 0.016$) is more than twenty times lower than that measured for the best sample ($A_{\text{PL}}/A_{\text{D}} = 0.33$) previously grown using the $\text{CH}_4\text{-CO}_2$ gas mixture [6], before optimising the experimental set-up.

The films grown at higher methane concentrations (up to 2.2% CH_4) show very high crystalline quality ($\text{FWHM} \leq 3\text{ cm}^{-1}$) and no evidence of graphitic or amorphous phases, although the photoluminescence background is slightly higher. It is important to note that the amplitudes of the broadband $\mu\text{-PL}$, commonly reported in the literature for diamond samples of quite good quality, are comparable or even greater than that of the diamond Raman line [8]. On the contrary, the amplitude of the broadband $\mu\text{-PL}$ measured in all our samples is always more than ten times lower than the diamond line amplitude, which once more clearly demonstrates the excellent quality of the diamond samples obtained after the optimisation of the experimental set-up.

4.2 Diamond-silicon interface

In order to investigate the dependence of the diamond grain quality along the growth direction, PL and Raman measurements were carried out at different focalisation depths of the laser beam within the film. Figure 4 shows the $\mu\text{-PL}$ spectrum taken on the same diamond grain as in Figure 3, but focusing the laser beam close to the D-Si interface. The sharp peak at about 520 cm^{-1} is due to the Raman scattering from the Si substrate. The broadening of the diamond Raman line ($\text{FWHM} = 3.6\text{ cm}^{-1}$) indicates a poorer crystalline quality close to the substrate interface, where the concentration of grain boundaries is higher [25].

As for the broadband PL at $\sim 2\text{ eV}$, the $A_{\text{PL}}/A_{\text{D}}$ ratio increases from 0.016 to about 0.16 moving from growth surface to the D-Si interface. Since a possible origin of this broad PL band is the amorphous sp^2 -type bonding [7,8], the increase of its intensity going towards the interface could indicate the presence of traces of sp^2 defects, not easily detectable through the Raman signature at 1500 cm^{-1} because of its very low intensity and the simultaneous presence of the wing of the PL band.

In all our samples a PL emission band at about 5880 cm^{-1} ($\sim 1.68\text{ eV}$) is detected as the laser beam is focused close to the interface (Fig. 4). This 1.68 eV feature is characteristic of CVD diamond films grown on Si substrates [15,27,28] and many models have been suggested for this center [29–33], all involving substitutional

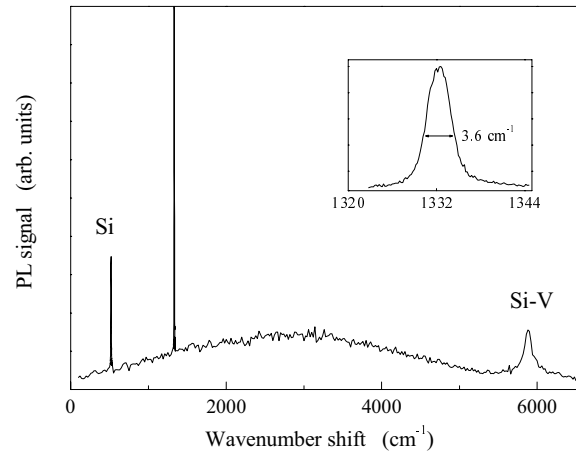


Fig. 4. Micro-PL spectrum taken on the same grain of Figure 3 but focusing at the film-substrate interface.

or interstitial Si-vacancy complex. The proposed formation mechanism [7] for this radiative center is based on the plasma-etching of the substrate during the early stages of the growth process. When the diamond grains coalesce to form a continuous film, no further etching of the substrate occurs and the incorporation of Si atoms into the growing film diminishes. According to this model, we find that the 1.68 eV PL intensity decreases going towards the growth surface, which confirms that the optical centres responsible for the 1.68 eV emission have higher concentration close to the substrate interface.

4.3 Macro-Raman and macro-PL measurements

The micro-sampling system utilised in this study is indispensable for monitoring the intrinsic quality of individual grains and analysing the spatial distribution of defects and impurities. However, in highly inhomogeneous samples such as polycrystalline CVD diamond films, Raman microscopy has the obvious disadvantage of providing strongly variable results from point to point within the sample [4]. Such a great variability may be a serious problem when one must compare different samples grown in almost the same experimental conditions, as for instance in case of a systematics. In order to be fully representative, the results obtained on a great deal of different grains should be properly averaged. The easiest and fastest means of performing this average is to make use of a macro sampling system. In the macro excitation mode, due to the great focus depth and large spot size of the laser beam, the response of diamond crystallites is averaged over the whole film thickness and over a circular area of about $100\text{ }\mu\text{m}$ diameter.

Due to grain boundaries, crystal defects and diamond-silicon lattice mismatch, individual crystallites within the film undergo different levels of internal stress, determining different shifts of the Raman peak position over the single-crystal value. The resulting spatial distribution of peak positions constitutes the principal mechanism of inhomogeneous broadening of the macro-Raman lines [5].

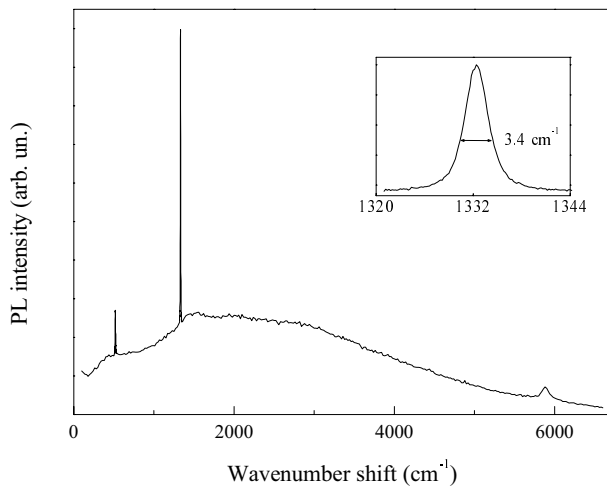


Fig. 5. Macro-PL spectrum of the diamond sample grown at 0.6% CH_4 in H_2 .

In our new samples, linewidths of about 3.4 cm^{-1} have been measured uniformly over the whole film surface. Such a narrow FWHM, although not surprising due to the very low values obtained both at the growth surface and the substrate interface, indicates a quite good global crystalline quality of the films. By comparison, the samples previously grown by using the $\text{CH}_4\text{-CO}_2$ gas mixture exhibit typical macro-Raman linewidth ranging from ~ 4 to $\sim 9 \text{ cm}^{-1}$ [6].

Figure 5 shows the macro-Raman (inset) and macro-PL spectra of the 0.6% CH_4 sample, whose “micro” spectra at the growth surface and interface are reported in Figures 3 and 4. Compared to the diamond peak, both the broad PL band and the weak non-diamond carbon band at $\sim 1500 \text{ cm}^{-1}$ are sensibly increased with respect to the “micro” measurements. In fact, in the macro mode the highly defective region close to the interface is entirely excited. Here the total area of grain boundaries, compared to the grain volume, is enormously greater than at the growth surface, due to the very small size of the diamond crystallites. As defects and non-diamond carbon phases are believed to be chiefly accumulated at the grain boundaries [7,34,35], the signals originating from grain boundary regions become more easily detectable. Due to both the film thickness and the high density of grain boundaries at the interface, the PL signal of the Si-related centre at 1.68 eV is hard to collect and appears as a very weak band at $\sim 5880 \text{ cm}^{-1}$ in relative scale.

We find that the intensity of the broad PL band centred at $\sim 2 \text{ eV}$ increases with increasing the methane concentration in the growth mixture. Figure 6 shows the PL spectra of a series of diamond samples grown with $\text{CH}_4\%$ in the range 0.6–2.2%. The ratio $A_{\text{PL}}/A_{\text{D}}$, reported in Figure 7, increases monotonically with increasing $\text{CH}_4\%$. An analogous trend is found in the ratio $A_{\text{ND}}/A_{\text{D}}$, although the numerical values are sensibly lower and more scattered. These results indicate that the quality of the diamond films deteriorates with increasing $\text{CH}_4\%$ [11,12],

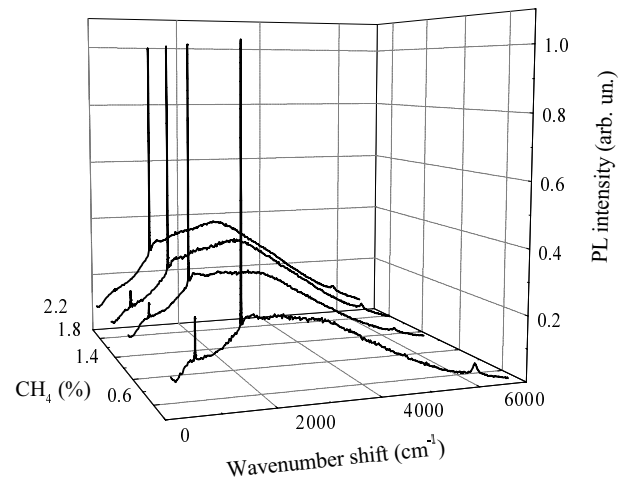


Fig. 6. Evolution of the macro-PL spectra with varying the CH_4 concentration in the $\text{CH}_4\text{-H}_2$ gas mixture.

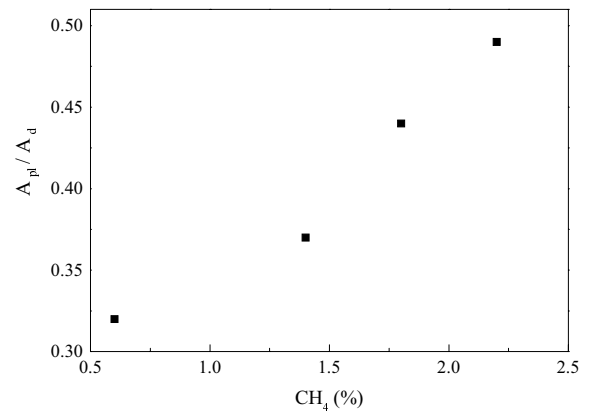


Fig. 7. Ratio $A_{\text{PL}}/A_{\text{D}}$ of the PL band amplitude to the diamond peak amplitude as a function of the CH_4 percentage in the $\text{CH}_4\text{-H}_2$ gas mixture.

because of the faster deposition rate occurring at higher methane concentrations.

Recently, the high quality of these films has been independently determined through their remarkable detection performance. In particular, efficiency data of α -particle detectors realised using these same diamond films show a decrease in detection efficiency at higher methane concentration, correlated to the lower global quality of the films evidenced by Raman and PL measurements [10].

5 Conclusions

In this paper, Raman spectroscopy and photoluminescence have been utilised to monitor the quality of synthetic diamond films grown by MWPECVD. A sensible improvement in the film quality has been obtained after the optimisation of the experimental set-up and of the growth parameters.

Micro-Raman analysis shows that linewidths of the diamond peak ranging from 2.1 to 3 cm^{-1} can be easily measured at the growth surface, indicating that the crystalline quality of individual grains is comparable or even superior to that of the best natural diamonds. These FWHM values are among the narrowest linewidths reported to date in continuous diamond films deposited onto non-diamond substrates. The excellent phase purity of the individual grains at the growth surface is witnessed by the complete absence of any non-diamond carbon feature at $\sim 1500 \text{ cm}^{-1}$ and by a very weak luminescence background.

Micro-Raman and μ -PL measurements carried out at different depths within the film show a worsening of the quality of the diamond particles going towards the D-Si interface, both in terms of diamond line broadening and of increase of PL background.

A 1.68 eV PL band, attributed to Si impurity, is observed close to the interface. The disappearing of this band moving towards the growth surface suggests that the concentration of the 1.68 eV defect is larger at the substrate side, providing support to the conclusion that the 1.68 eV centre originates by plasma etching of the Si substrate [7, 8].

The progressive enhancement of the methane concentration in the gas mixture determines a worsening in the film quality, witnessed by an increase of the broadband PL at about 2 eV.

Our experimental results show that the interface zone is highly defective, due to the presence of small size diamond particles, high density of grain boundaries and Si impurities. The comparison with the results obtained onto the growth surface suggests that, in our experimental conditions, the basic limitation to an excellent global quality of the diamond films is not related to the growth parameters, which seem to be quite well optimised, but rather to the presence of a highly defective interface layer. Thus, excellent quality films for advanced applications should be easily obtained by simply increasing the film thickness and by removing the poor quality interface layer.

References

1. D.S. Knight, W.B. White, *J. Mater. Res.* **4**, 385 (1989).
2. P.K. Bachmann, D.U. Wiechert, *Diam. Relat. Mater.* **1**, 422 (1992).
3. R.J. Nemanich, J.T. Glass, G. Lucovsky, R.E. Shroder, *J. Vac. Sci. Technol. A* **6**, 1783 (1988).
4. Y. von Kaenel, J. Stiegler, J. Michler, E. Blank, *J. Appl. Phys.* **81**, 1726 (1997).
5. M.G. Donato, G. Faggio, M. Marinelli, G. Messina, E. Milani, A. Paoletti, S. Santangelo, A. Tucciarone, G. Verona Rinati, *A joint macro-/micro- Raman investigation of the diamond lineshape in CVD diamond films: the influence of texturing and stress*, *Diam. Relat. Mater.* (to be published).
6. G. Faggio, M. Marinelli, G. Messina, E. Milani, A. Paoletti, S. Santangelo, A. Tucciarone, G. Verona Rinati, *Diam. Relat. Mater.* **8**, 640 (1999).
7. L. Bergman, B.R. Stoner, K.F. Turner, J.T. Glass, R.J. Nemanich, *J. Appl. Phys.* **73**, 3951 (1993).
8. L. Bergman, M.T. McClure, J.T. Glass, R.J. Nemanich, *J. Appl. Phys.* **76**, 3020 (1994).
9. R. Di Benedetto, M. Marinelli, G. Messina, E. Milani, E. Pace, A. Paoletti, A. Pini, S. Santangelo, S. Scuderi, A. Tucciarone, G. Verona Rinati, G. Bonanno, *11th European Conference Diamond 2000, Porto (Portugal), 3-8 September 2000*.
10. M.G. Donato, G. Faggio, M. Marinelli, G. Messina, E. Milani, A. Paoletti, S. Santangelo, A. Tucciarone, G. Verona Rinati, *High quality CVD diamond for detection applications: structural characterisation*, *Diam. Relat. Mater.* (to be published).
11. Y.K. Kim, K.Y. Lee, J.Y. Lee, *Thin Solid Films* **272**, 64 (1996).
12. S.M. Leeds, T.J. Davis, P.W. May, C.D.O. Pickard, M.N.R. Ashfold, *Diam. Relat. Mater.* **7**, 233 (1998).
13. G. Lippold, D. Aderhold, F.J. Comes, W. Grill, *Diam. Relat. Mater.* **6**, 1587 (1997).
14. T.S. McCauley, Y.K. Vohra, *Phys. Rev. B* **49**, 5046 (1994).
15. J. Rosa, J. Pangrac, M. Vanecek, V. Vorlicek, M. Nesladek, K. Meykens, C. Quaeys, L.M. Stals, *Diam. Relat. Mater.* **7**, 1048 (1998).
16. M.C. Rossi, S. Salvatori, F. Galluzzi, F. Somma, R.M. Montereali, *Diam. Relat. Mater.* **7**, 255 (1998).
17. J.W. Ager III, M.D. Drory, *Phys. Rev. B* **48**, 2691 (1993).
18. S.A. Stuart, S. Praver, P.S. Weiser, *Appl. Phys. Lett.* **62**, 1227 (1993).
19. M.C. Rossi, *Appl. Phys. Lett.* **73**, 1203 (1998).
20. R. Linares, P. Doering, *Diam. Relat. Mater.* **8**, 909 (1999).
21. Y. Sato, M. Kamo, *Surf. Coat. Technol.* **39/40**, 183 (1989).
22. S. Praver, A. Hoffman, S.A. Stuart, R. Manory, P. Weiser, *J. Appl. Phys.* **69**, 6625 (1991).
23. K. Iakoubovskii, A. Stesmans, G.J. Adriaenssens, R. Provoost, R.E. Silverans, V. Raiko, *Phys. Stat. Sol. (a)* **174**, 137 (1999).
24. S.E. Coe, R.S. Sussmann, *Diam. Relat. Mater.* **9**, 1726 (2000).
25. C. Jany, A. Tardieu, A. Gicquel, P. Bergonzo, F. Foulon, *Diam. Relat. Mater.* **9**, 1086 (2000).
26. D. Meier, *Diamond Detectors for Particle Detection and Tracking*, Ph.D. thesis, University of Heidelberg (1999).
27. T. Feng, B.D. Schwartz, *J. Appl. Phys.* **73**, 1415 (1993).
28. M.C. Rossi, S. Salvatori, F. Galluzzi, *Diam. Relat. Mater.* **6**, 712 (1997).
29. V.S. Vavilov, A.A. Gippius, A.M. Zaitsev, B.V. Deryagin, B.V. Spitsyn, A.E. Aleksenko, *Sov. Phys. Semicond.* **14**, 1078 (1980).
30. P.J. Lin-Chung, *Phys. Rev. B* **50**, 16905 (1994).
31. C.D. Clark, H. Kanda, I. Kiflawi, G. Sittas, *Phys. Rev. B* **51**, 16681 (1995).
32. J.P. Goss, R. Jones, S.J. Breuer, P.R. Briddon, S. Öberg, *Phys. Rev. Lett.* **77**, 3041 (1996).
33. L. Bergman, R.J. Nemanich, *J. Appl. Phys.* **78**, 6709 (1995) and references therein.
34. L.C. Nistor, J. Van Landuyt, V.G. Ralchenko, A.A. Smolin, K.G. Korotushenko, E.D. Obraztsova, *J. Mater. Res.* **12**, 2533 (1997).
35. L.C. Nistor, J. Van Landuyt, V.G. Ralchenko, E.D. Obraztsova, A.A. Smolin, *Diam. Relat. Mater.* **6**, 159 (1997).